Energy & Environmental Science

PAPER

View Article Online
View Journal | View Issue

CrossMark click for updates

Cite this: *Energy Environ. Sci.*, 2015, **8**, 975

Platinum(II)–porphyrin as a sensitizer for visible-light driven water oxidation in neutral phosphate buffer†

Hung-Cheng Chen, Dennis G. H. Hetterscheid,‡ René M. Williams, Jarl Ivar van der Vlugt, Joost N. H. Reek* and Albert M. Brouwer*

Received 18th October 2014
Accepted 2nd January 2015

DOI: 10.1039/c4ee03302g

www.rsc.org/ees

A water-soluble Pt(II)–porphyrin with a high potential for one-electron oxidation (~1.42 V *vs.* NHE) proves very suitable for visible-light driven water oxidation in neutral phosphate buffer solution in combination with a variety of water oxidation catalysts (WOCs). Two homogeneous WOCs (iridium(N-heterocyclic carbene) and Co_4O_4–cubane complexes) and two heterogeneous WOCs ($IrOx{\cdot}nH_2O$ and Co_3O_4 nanoparticles) were investigated, with sodium persulfate ($Na_2S_2O_8$) as a sacrificial electron acceptor. Under neutral buffer conditions, the Pt(II)–porphyrin shows higher stability than the commonly used photosensitizer $[Ru(bpy)_3]^{2+}$, and therefore represents a good alternative photosensitizer to be used in the evaluation of light driven WOCs.

Broader context

Making fuels *via* artificial photosynthesis is viewed as one of the most promising ways to produce clean and sustainable energy. In this approach, electrons are taken from water and transferred to electron acceptors, for example protons, which are then reduced to hydrogen. Oxidation of water leads to oxygen as a stable product in a four-electron process. Catalysts are required to make this complex reaction proceed at acceptable rates at low temperatures. Another key element for photochemical water oxidation is the photosensitizer, which utilises the excitation energy, harvested from sunlight, to oxidize the catalyst. The evaluation of new catalysts for water oxidation is often carried out in a test system involving persulfate as a sacrificial electron acceptor and $Ru(bpy)_3^{2+}$ as the photosensitizer. This photosensitizer has several drawbacks. It can only be used with specific buffers and pH ranges, absorbs only a small fraction of the solar spectrum, and is not very stable under prolonged illumination. In this report, we demonstrate a water-soluble Pt–porphyrin photosensitizer, Pt(II)–TCPP that performs much better than $Ru(bpy)_3^{2+}$. It works well in concentrated neutral phosphate buffer solution and because of its higher oxidizing power it can activate a wide range of (water oxidation) catalysts.

1. Introduction

Solar-to-fuel approaches potentially provide a solution for the increasing human energy requirement.[1,2] One of the options is solar-driven water splitting to produce O_2 and H_2 by means of photoelectrochemical cells.[3–6] Such cells include components for light harvesting, for light-driven water oxidation (a mimic of photosystem II (PSII)) and for proton reduction (a mimic of photosystem I (PSI)).

For the fabrication of working (nanoscale molecular) devices the individual elements need to be integrated by using immobilization technology.[7–9]

Although the driving force for the overall water splitting reaction is independent of pH, this is not true for the half-reactions. The potential for water oxidation is $E^0(O_2/H_2O) = 1.23–0.059 \times$ pH V *vs.* NHE,[10] so higher pH results in a lower oxidation potential. Proton reduction, on the other hand, is more difficult at high pH.[11] Consequently, considering an integrated photocatalytic water splitting device with both half-reactions coupled in a photo-electrochemical cell, neutral pH conditions are favourable in order to balance these counter-acting effects.

Typically, the half-reactions are studied and optimized separately. For water oxidation, three-component systems composed of a photosensitizer (PS), a sacrificial electron acceptor and a catalyst (WOC) are often employed.[12–14] Because the singlet excited states of photosensitizers are usually too short-lived for an efficient diffusion-limited reaction with the electron acceptor, long-lived triplet state photosensitizers are preferred in order to efficiently generate radical cations in solution.[15,16] Redox-level matching is another key requirement for efficient photocatalytic water oxidation.[14,17,18]

Van't Hoff Institute for Molecular Sciences, University of Amsterdam, P.O. Box 94157, 1090 GD Amsterdam, The Netherlands. E-mail: A.M.Brouwer@uva.nl

† Electronic supplementary information (ESI) available: Experimental procedures, including procedures for photophysical, electrochemistry and oxygen evolution measurements; additional Fig. S1–S20. Quantum yield determination; synthesis of photosensitizers and catalysts, and sample preparation. See DOI: 10.1039/c4ee03302g

‡ Present address: Faculty of Science, Leiden Institute of Chemistry, Einsteinweg 55, P.O. Box 2333 CC Leiden, The Netherlands.

Ruthenium polypyridine complexes are among the most commonly used photosensitizers in photocatalytic water oxidation,[13,19,20] with *tris*(2,2′-bipyridyl)ruthenium(II), $[Ru(bpy)_3]^{2+}$, as the archetypical proponent.[21,22] Metalloporphyrins have also been reported for light-driven water oxidation, given their broad spectral absorption, high triplet-state yield and long-lived radical cations in solution.[16] Most metalloporphyrins, however, have potentials of one-electron oxidation similar to that of $[Ru(bpy)_3]^{2+}$,[23,24] limiting their application as photosensitizers to low overpotential WOCs or to high pH media.[18,25,26] For both PS classes, modification of the ligand structure may increase the redox potential,[27,28] which broadens the scope of photocatalytic WOC-systems.[29,30]

Catalytic water oxidation leads to progressive acidification of the reaction medium at higher conversion, resulting in less favourable thermodynamics. Moreover, proton-coupled electron-transfer (PCET) plays a key kinetic role in these mechanisms.[31,32] As water is a poor proton acceptor at pH 7, phosphate has been added as an effective proton acceptor.[33–35] Several water oxidation catalysts have been reported that catalyze water electrolysis[36–39] or chemical oxidation[40] in neutral phosphate buffer solution. However, $[Ru(bpy)_3]^{2+}$ is incompatible with this reaction medium because of rapid photobleaching and photo-decomposition.[41,42] To improve photostability, weakly nucleophilic inorganic Na_2SiF_6–$NaHCO_3$ buffer systems at pH = 5.30–5.75 have been introduced in connection to Ru–PS systems.[41,43,44] Unfortunately, these silicate buffers are unstable, leading to oligomeric silicates or colloidal silica at near neutral pH.[45,46]

Hence, there is a demand for long-lived photostable photosensitizers with intense visible-light absorption and high formal potential to initiate photocatalytic water oxidation in concentrated (>0.1 M) phosphate buffer solution at pH 7.0. Recently, Pt(II)–porphyrins were reported with high $E_{1/2}(Pt^{III/II})$ redox potentials.[47] Herein, we report the photocatalytic water oxidation by a water-soluble Pt(II)–porphyrin photosensitizer, Pt(II)–TCPP (Fig. 1) applied in combination with both homogeneous (Ir–NHC (ref. 48) and Co_4O_4–cubane complexes[19]) and heterogeneous WOCs ($IrO_x \cdot nH_2O$ ~2 nm (ref. 49) and Co_3O_4 nanoparticles, ~50 nm)[50] in neutral phosphate buffer solution. We demonstrate that Pt(II)–TCPP is a readily available, stable and superior photosensitizer compared to $[Ru(bpy)_3]^{2+}$ for WOCs with overpotentials in the range of 350–500 mV in concentrated neutral phosphate buffer.

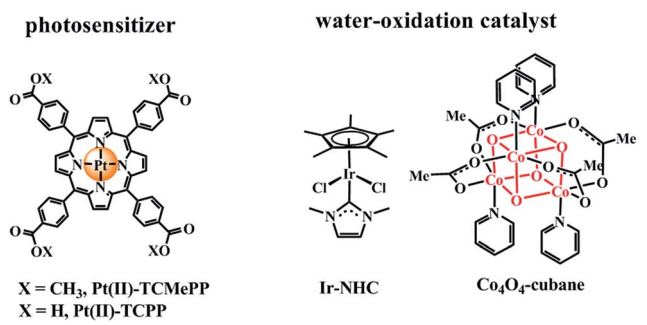

Fig. 1 Chemical structures of the Pt(II)–porphyrin photosensitizers Pt(II)–TCMePP, Pt(II)–TCPP and two homogeneous water oxidation catalysts: Ir–NHC, Co_4O_4–cubane used in this study.

2. Results and discussion

2.1 Steady-state absorption and emission measurements

To determine the potential efficacy of Pt–porphyrins as photosensitizers for WOC chemistry, we investigated the photochemistry of the tetracarboxylic acid Pt(II)–TCPP in phosphate buffer. For comparison, some measurements of the corresponding methyl ester Pt(II)–TCMePP in dichloromethane are included.[51] The steady-state absorption spectra are depicted in Fig. 2(a). The absorption spectrum of Pt(II)–TCMePP consists of a high-energy B-band (401 nm, $\varepsilon = 2.6 \times 10^5$ M^{-1} cm^{-1}) and lower energy Q-bands (511 nm, $\varepsilon = 2.4 \times 10^4$ M^{-1} cm^{-1}; 540 nm, $\varepsilon = 6.0 \times 10^3$ M^{-1} cm^{-1}). For Pt(II)–TCPP in phosphate buffer solution, the B-band is at 395 nm ($\varepsilon = 2.1 \times 10^5$ M^{-1} cm^{-1}) and the Q-bands are at 511 nm ($\varepsilon = 1.7 \times 10^4$ M^{-1} cm^{-1}) and 542 nm ($\varepsilon = 2.7 \times 10^3$ M^{-1} cm^{-1}).

The triplet state energy was determined with steady state luminescence spectroscopy in solution (deoxygenated by N_2 purging) at ambient temperature (21 °C). The emission spectra of the two Pt(II)–porphyrins are shown in Fig. 2(b). The emission maxima are strongly shifted from 652 nm for Pt(II)–TCMePP in dichloromethane to 681 nm for Pt(II)–TCPP in phosphate buffer solution. The stronger solute/solvent interaction in water apparently lowers the energy of the triplet excited state. As a conservative estimate, we take the position of the first peak as a measure of the triplet energy ($E(T_1) \geq 1.82$ eV). The luminescence decay time was found to be 2.2 μs in air-saturated solution, and 9 μs after purging with argon, in agreement with the triplet nature of the emitting species (Fig. S1, ESI†). The triplet lifetime of $[Ru(bpy)_3]^{2+}$ is ~0.58 μs in deaerated water at room temperature,[52] even shorter than that of Pt(II)–TCPP in air-saturated solution.

2.2 Electrochemical characterization

The cyclic voltammogram of Pt(II)–TCMePP in dichloromethane (Fig. S2, ESI†) shows two reversible one-electron oxidation and reduction waves with half-wave potentials $E_{1/2}(Pt^{III/II}) = 1.50$ and $E_{1/2}(Pt^{I/II}) = -1.00$ V *vs.* NHE, respectively. $E_{1/2}(Pt^{III/II})$ is 0.67 V higher than that of water $E^0(O_2/H_2O)$

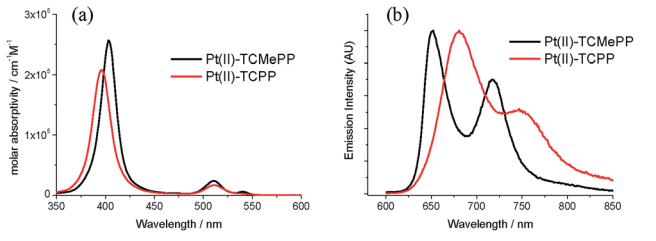

Fig. 2 (a) Absorption spectra of Pt(II)–TCMePP (black) in dichloromethane and Pt(II)–TCPP (red) in phosphate buffer (0.1 M, pH = 7.0) solution. (b) Emission spectra upon 540 nm excitation at room temperature in the corresponding solvents.

at pH = 7, which shows that Pt(II)–TCMePP can potentially be used as a PS coupled to WOCs with moderate-to-high overpotentials under neutral conditions. Furthermore, in order to establish the redox-level matching between Pt(II)–TCTPP and the envisioned WOC systems, cyclic voltammetry was performed in a NaH_2PO_4/Na_2HPO_4 buffer at pH 7.0 (Fig. 3). The oxidation of Pt(II)–TCPP at 1.42 V (*vs.* NHE) is poorly reversible, in line with that reported for other water soluble metalloporphyrins.[23,26] There is little difference between the E_{ox} of Pt(II)–TCMePP in the organic solvent and the value obtained for Pt(II)–TCPP in water. Importantly, this formal potential of Pt(II)–TCPP is more positive than the relevant onset potentials for water oxidation of all WOCs investigated in the present study, implying that (photo)oxidized Pt(II)–TCPP is thermodynamically capable to activate these WOCs by electron transfer in neutral phosphate buffer. Using Ir–NHC as the WOC, the onset for electrocatalysis is observed around 1.20 V, resulting in an overpotential of 380 mV at pH 7, which is similar to those of other mononuclear Ir-based WOCs in neutral water.[53] The Co_4O_4–cubane system is electrocatalytically active from 1.32 V onwards, implying an overpotential of 500 mV, similar to reported values.[14,54] The electrocatalytic properties of iridium–oxide nanoparticles are shown in Fig. 3(c). The concentration of the $IrO_x{\cdot}nH_2O$ nanoparticles was calculated by using the extinction coefficient of 630 cm^{-1} M^{-1} at 580 nm.[49] The onset electrocatalytic potential is near 1.15 V for the $IrO_x{\cdot}nH_2O$ nanoparticles. Compared to other electrocatalytic studies of iridium oxide systems, our ligand-free $IrO_x{\cdot}nH_2O$ nanoparticles in neutral phosphate electrolyte solution show a similar overpotential of 330 mV as reported for succinate stabilized $IrO_x{\cdot}nH_2O$.[45,55] The electrocatalytic potential of the Co_3O_4 nanoparticles was not studied because the suspension does not permit homogeneous diffusion near the working electrode surface. Therefore, we estimated the overpotential to be 350 mV for the Co_3O_4 particles using the work of Jiao and Frei.[56]

The photophysical and electrochemical data were used to construct energy level diagrams including combinations of WOC, PS and sacrificial electron acceptor ($Na_2S_2O_8$) in phosphate buffer at pH 7.0 (Fig. 4). Highly exothermic triplet-state one-electron transfer ($\Delta G = -1.01$ eV) from photogenerated ^{3}Pt(II)–TCPP ($E_{1/2}(Pt^{III/II}) = -0.40$ V) to $S_2O_8^{2-}$ in buffer solution[16] results in formation of the Pt(II)–porphyrin radical cation.

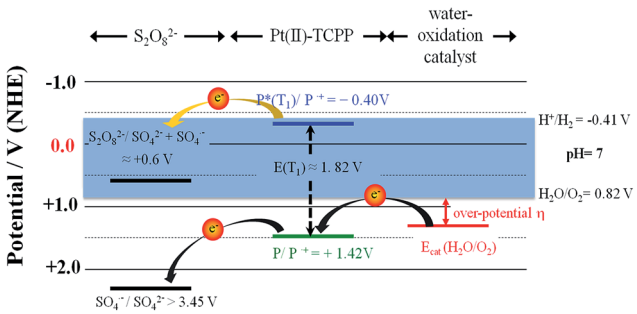

Fig. 4 Energy scheme of Pt(II)–TCPP and water oxidation catalysts. Overpotential η: 380 mV for Ir–NHC, 500 mV for Co_4O_4–cubane, 330 mV for $IrO_x{\cdot}nH_2O$ nanoparticles and 350 mV for Co_3O_4 nanoparticles in phosphate buffer (0.2 M, pH = 7.0) solution.

This species ($E_{red} = 1.42$ V) is thermodynamically capable of driving WOCs to oxidize water to O_2. The $SO_4^{\cdot-}$ released in the one-electron reduction can oxidize the ground state of Pt(II)–TCPP, or the WOC if present in sufficiently high concentration.[15]

2.3 Light-driven water oxidation: oxygen generation in neutral phosphate buffer solution

Photocatalytic water oxidation experiments were carried out in solutions containing 6.7×10^{-4} M Pt(II)–TCPP and 5.0×10^{-2} M $Na_2S_2O_8$ in phosphate buffer solution (0.1 M, pH = 7.0) at room temperature. Photocatalytic oxygen generation was monitored through the detection of dissolved O_2 using a Clark-type electrode. A 120 W halogen lamp was used as the irradiation source. The results of light-driven oxygen formation with different WOCs are shown in Fig. 5. Because the WOC employed may not be the actual catalytically active species,[57,58] turnover numbers and frequencies are of limited value. For the interested reader the values obtained assuming that the molecular catalysts react as such are given in the ESI.† As shown in Fig. 5, gradually growing [O_2] was observed in all photocatalytic reactions after the light was switched on after ~2 minutes. Control experiments were performed in which each individual component of the system was removed. Significant oxygen generation was only observed when all three components were present (see ESI,

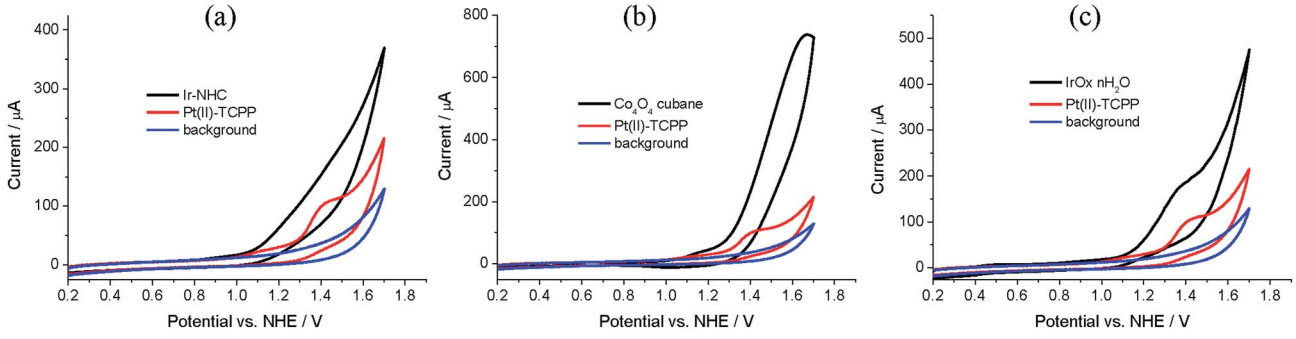

Fig. 3 Cyclic voltammograms of (a) Ir–NHC (1 mM), (b) Co_4O_4–cubane (1 mM), (c) $IrO_x{\cdot}nH_2O$ nanoparticles (1.9 mM) compared with Pt(II)–TCPP (1 mM; red curves) and the NaH_2PO_4/Na_2HPO_4 (0.2 M, pH = 7.0) electrolyte background (blue curves).

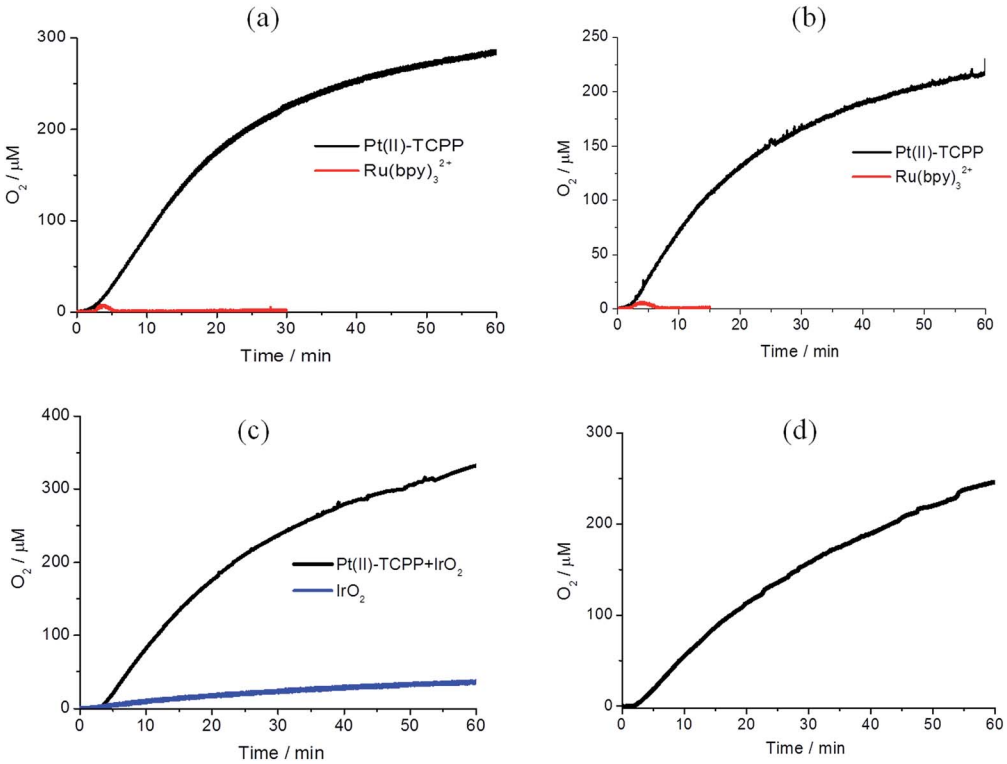

Fig. 5 Photochemical oxygen evolution in 1.5 mL of pH 7.0, 0.1 M phosphate buffer solutions containing $Na_2S_2O_8$ (5.0×10^{-2} M), Pt(II)–TCPP (6.7×10^{-4} M) and catalysts: (a) Ir–NHC (5.0×10^{-5} M), (b) Co_4O_4–cubane (5.0×10^{-5} M), (c) $IrO_x \cdot nH_2O$ nanoparticles (1.8×10^{-4} M) and (d) Co_3O_4 nanoparticles (4.16×10^{-5} g mL^{-1}). The red lines in (a) and (b) are obtained with $Ru(bpy)_3^{2+}$ (6.7×10^{-4} M) as the photosensitizer and the blue line in (c) is the control experiment without Pt(II)–TCPP.

Fig. S5†). Noteworthy, our $IrO_x \cdot nH_2O$ nanoparticles show a non-sensitized water oxidation with a low O_2 evolution in the control experiment in Fig. 5(c).[59]

In order to make a comparison of photocatalytic activity between Pt(II)–TCPP and $Ru(bpy)_3^{2+}$, we also studied the photocatalytic reaction of $Ru(bpy)_3^{2+}$ under the same reaction conditions. The results are shown by the red lines in Fig. 5(a) and (b), respectively, and in Fig. S6.† As expected, these photocatalytic oxygen generations came to a halt within three minutes. It is well known that $Ru(bpy)_3^{2+}$ is not photostable in the presence of persulfate in high concentration phosphate containing buffer.[41] Moreover, the bipyridine ligand of $Ru(bpy)_3^{2+}$ can be rapidly oxidized to CO_2 in high concentration $Na_2S_2O_8$ with or without WOCs in borate buffer.[58] This explains why the O_2 concentration rapidly decreased after a few minutes of illumination. In contrast, Pt(II)–TCPP is photochemically stable for more than one hour under photocatalytic reaction conditions. It can be concluded that Pt(II)–TCPP reveals greatly enhanced photostability during light-driven water oxidation in phosphate buffer solution compared to $Ru(bpy)_3^{2+}$. In order to address the photostability of both photosensitizers in the photocatalytic reaction, the UV-vis absorptions can be used to follow the decomposition (see ESI, Fig. S13 and S14†).[27] In the case of $Ru(bpy)_3^{2+}$, the absorbance of the MLCT band at 452 nm was followed as a function of time. The rapidly decreased absorbance indicates that more than 50% was already decomposed after illuminating for five min. In the case of Pt(II)–TCPP on the other hand, only approximately 3% was decomposed after the same illumination time, according to the reduction of the Q-band absorption at 515 nm. The major photodegradation pathways of water-soluble porphyrins have been studied intensively. It has been shown that the π-radical cation of porphyrins can undergo nucleophilic addition of hydroxide ions at the *meso* position, whereupon it is converted to isoporphyrin derivatives such as hydroxyphlorin, and further to ring-opened bilinone derivatives.[60] However, the absorption spectra of these degraded products (hydroxyphlorins, in particular) were not observed in our Pt(II)–TCPP photocatalytic reaction mixtures.[61,62] The four negatively charged peripheral benzoate groups stabilize the positive charge of the π-radical cation. Similar effects have been observed for *meso*-tetrakis(4-sulfonatophenyl)porphyrins.[18,63] We further compared the changes in the absorption spectra of irradiated solutions of PS and persulfate in the absence and presence of a WOC (Fig. S15†). Photodegradation is notably slower in the presence of the WOC. This finding suggests that electron transfer from the WOC to PS radical cation favorably competes with its degradation reactions.

$Ru(bpy)_3^{2+}$ can show light driven water oxidation activity for a longer time in the Na_2SiF_6–$NaHCO_3$ buffer system, which was extensively studied in the literature.[41,43,56] Recently, Hill *et al.* also reported the long time light driven water oxidation with

$Ru(bpy)_3^{2+}$ and a cobalt-based polyoxometalate complex as a water oxidation catalyst in the weakly nucleophilic $Na_2B_4O_7$ buffer.[64] Compared to the same lower concentration of borate and phosphate buffer (pH = 8.0 and 20 mM, respectively), the borate buffer easily loses its buffer function. A high borate buffer concentration (80 mM, pH = 8.0) can maintain the pH in the water oxidation period. The disadvantage of borate buffer is that it is only suitable for pH ≧ 8. In high pH solution, OH^- can also attack the bipyridine ring of $Ru(bpy)_3^{3+}$.[41,42] An improvement was reported by Sun *et al.*[27] The attachment of electron withdrawing moieties to the bipyridine not only increased E_{ox} but also improved the photostability of Ru–polypyridine photosensitizers in neutral phosphate buffer solution. This modified Ru–polypyridine photosensitizer was used to study long time photocatalytic reaction in neutral phosphate buffer solution (0.1 M, pH = 7.2) by Åkermark *et al.* recently.[30]

2.4 Illumination power dependence of light-driven water oxidation

The Ir–NHC, Co_4O_4–cubane and $IrO_x \cdot nH_2O$ nanoparticles show similar rates of O_2 formation under 120 W halogen lamp illumination as discussed in the previous section. In order to investigate whether the oxygen formation rates are limited by the photon absorption rate or the inherent catalytic activity of WOCs, the light-driven water oxidation activities were measured at different excitation powers (5.2 mW, 21.2 mW and 51.6 mW) of incident 532 nm laser light. The results of light-driven oxygen formation with different WOCs are shown in Fig. 6. Higher O_2 generation rates were obtained with an increasing incident light power from 5.2 mW to 21.2 mW with all WOCs. In all cases, however, the increase in O_2 generation rate does not match the increase in power. Upon further increasing the power of incident laser up to 51.6 mW, the oxygen generation rate even decreased in the cases of Ir–NHC, Co_4O_4–cubane and Co_3O_4 nanoparticles. The O_2 generation rate increased only for the $IrO_x \cdot nH_2O$ nanoparticles.

Several factors can be envisaged that may explain why the rate of formation of oxygen does not increase linearly with the excitation power. Most likely, the catalytic cycle is too slow to keep up with the excitation rate. A similar conclusion was also reached in the work of Jiao and Frei.[56] A more detailed kinetic study could shed more light on this, but this is outside the scope of the present paper. If the reduction of the radical cation of the PS by the WOC is rate limiting, side reactions of the radical cation may be relatively enhanced, which can speed up photodegradation and contribute to a smaller TON.

From the ratio of the absorbed photon flux and the rate of oxygen formation, the quantum yield of water oxidation $\Phi(H_2O)$ can be estimated to be 1.1% for Ir–NHC and Co_4O_4–cubane, and 0.6% for $IrO_x \cdot nH_2O$ and Co_3O_4 nanoparticles. These quantum efficiencies are probably underestimated, because the photon loss by reflection of incident light that passes through the cooling water mantle of the reaction vessel and light scattering of the nanoparticle suspension are not taken into account.

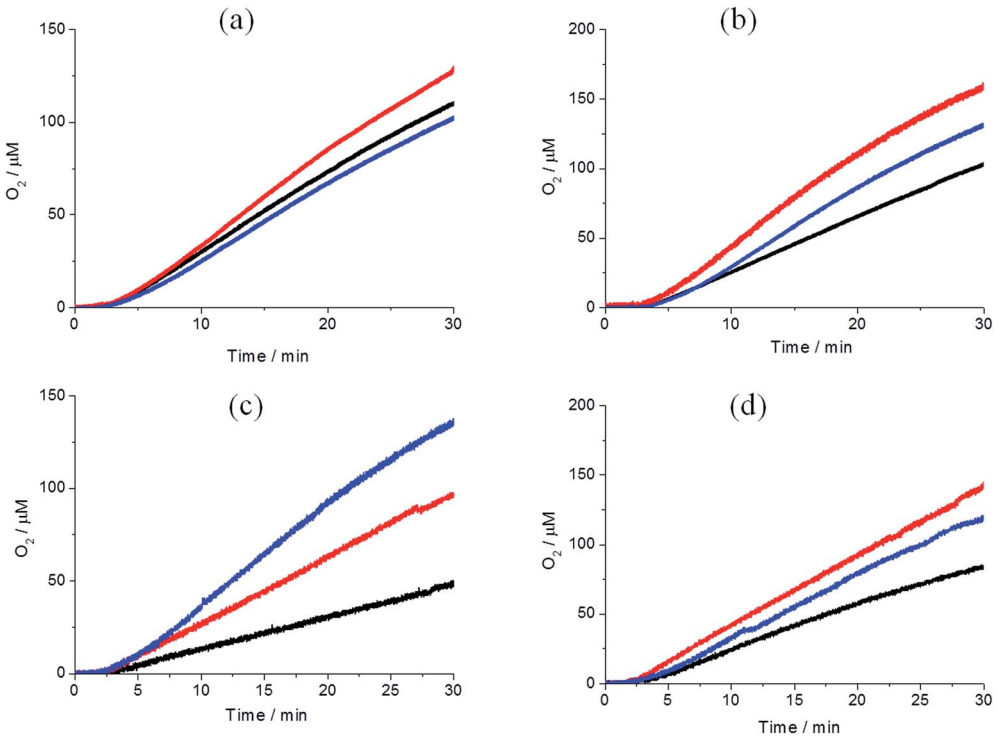

Fig. 6 Photochemical water oxidation with different excitation powers (black = 5.2 mW, red = 21.2 mW, and blue = 51.6 mW) of 532 nm green laser. Volume = 1.5 mL, pH 7.0, 0.1 M phosphate buffer, containing $Na_2S_2O_8$ (1.67×10^{-2} M), Pt(II)–TCPP (2.23×10^{-4} M) and catalysts: (a) Ir–NHC (1.67×10^{-5} M), (b) Co_4O_4–cubane (1.67×10^{-5} M), (c) $IrO_x \cdot nH_2O$ nanoparticles (6.00×10^{-5} M) and (d) Co_3O_4 nanoparticles (1.39×10^{-5} g mL^{-1}).

2.5 The advantages of a Pt(II)–porphyrin photosensitizer for sunlight driven water oxidation

One of the essential properties of chromophores applied to molecule-based artificial photosynthetic devices is their ability to capture photons over a large part of the solar spectrum. For example, the absorption wavelength of a recently proposed radically reengineered photosynthesis tandem photocell for light-driven water oxidation at pH = 7.0 was extended to 730 nm.[65] Fig. 7(a) shows the UV-vis spectra of the three chromophores: Pt(II)-TCMePP, $Ru(bpy)_3^{2+}$, and Chl *a* (related to the monomer of P680 in natural oxygenic photosynthesis[66]). In addition, Fig. 7(b) shows the calculated photon absorption rates of the three chromophores (2 μM solutions) under AM1.5G sunlight in the range of 300–730 nm.[67] The integrated molar absorptivities and percentages of photons absorbed by 2 μM chromophore solutions are shown in Table 1. Both values of Pt(II)–TCMePP are at least three times larger than those of $Ru(bpy)_3^{2+}$ because Pt(II)–TCMePP shows a much more intense absorption in the visible light range. Another parameter representing the photo-absorption ability of a chromophore is the 50% photon capture threshold (PCT^{50}),[67] which is the concentration of a chromophore needed to absorb 50% of incident solar photons in the given solar spectrum range. The PCT^{50} of Pt(II)–TCMePP is about one-third of that of $Ru(bpy)_3^{2+}$. Pt(II)–TCMePP exhibits a comparable integrated molar absorptivity relative to that of chlorophyll *a* due to the intense B-band transitions of the porphyrin chromophore. The photon absorption rate of 2 μM Pt(II)–TCMePP is also close to that of chlorophyll *a*. However, the PCT^{50} of chlorophyll *a* in the 300−730 nm solar spectrum is three times smaller than that of Pt(II)–TCMePP because the former has broader transitions that span a larger portion of the sunlight spectrum.

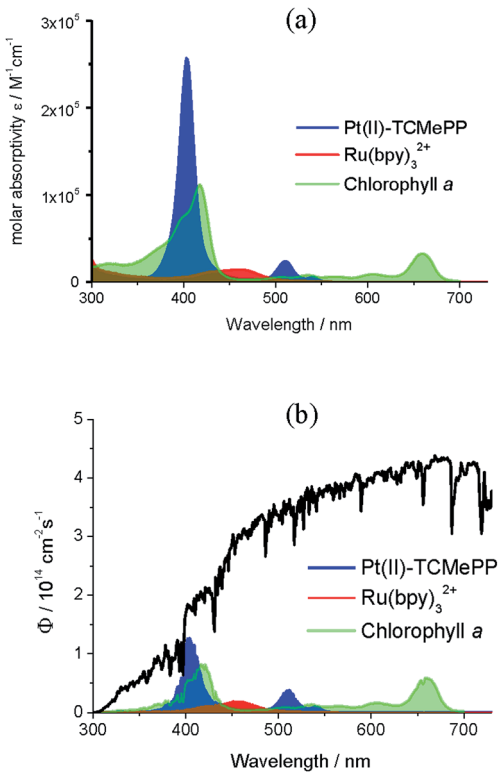

Fig. 7 (a) UV-vis spectra and (b) solar irradiance photon flux AM1.5G (black) and photon absorption rate for 2 μM solution of Pt(II)–TCMePP (blue), $Ru(bpy)_3^{2+}$ (red), chlorophyll *a* (green) in a 1 cm path length cell.

The second essential property of a photosensitizer for light-driven water oxidation is the first redox potential for oxidation. The $E_{1/2}(Pt^{III/II})$ of Pt(II)–TCMePP is 200 mV higher than $E_{1/2}(Ru^{III/II})$ of widely used $Ru(bpy)_2(4,4'\text{-}(PO_3H_2)_2bpy)^{2+}$ with anchoring phosphonic acid group in a dye-sensitized photoelectrochemical cell.[68] Thus, choosing Pt(II)–porphyrin as the photosensitizer for light-driven water oxidation not only affords a better light harvesting function under solar excitation but also provides a larger driving force for electron transfer from the WOC to the radical cation of the photosensitizer. For a WOC with a modest overpotential of 400 mV at pH 7.0, the free energy of electron transfer is only −80 mV when using $Ru(bpy)_2(4,4'\text{-}(PO_3H_2)_2bpy)^{2+}$ as the photosensitizer. However, the driving force for electron transfer can be improved to −280 mV by using Pt(II)–TCMePP. It has been reported for a ruthenium polypyridyl dye coupled to $IrO_x\cdot nH_2O$ catalytic particles (used in a dye-sensitized photoelectrochemical cell), that the slow electron transfer from the catalyst to the oxidized dye caused the low quantum efficiency.[44] Clearly, an increased electron transfer rate due to the higher reduction potential of the oxidized dye (and a larger driving force) of Pt(II)–TCMePP can be an important factor in enhancing the efficiency of the water oxidation

Table 1 Photo-absorption properties[a] of representative chromophores referenced to AM1.5G solar irradiance photon flux and their redox potentials

Molecule	Integrated molar absorptivity[b] (M^{-1})	AM1.5G photon capture[c] (2 μM)	50% photon capture threshold (PCT^{50})[d]	Redox potential *V vs.* NHE
Pt(II)–TCMePP	4.5×10^8	6.0%	122 μM	1.50
$Ru(bpy)_3^{2+}$	1.2×10^8	1.7%	360 μM	1.26[e]
Chlorophyll *a*	4.8×10^8	7.2%	38 μM	0.82[f,g]
P680				1.25[h]
$Ru(bpy)_2(4,4'\text{-}(PO_3H_2)_2bpy)^{2+}$				1.30[i]

[a] 300–730 nm. [b] The absorption spectra of $Ru(bpy)_3^{2+}$ and chlorophyll *a* are from ref. 70. [c] Percentage of incident solar photons absorbed for a solution of a given concentration (1 cm path length). [d] Concentration required to absorb 50% of the incident solar photons (1 cm path length). [e] Ref. 20. [f] Ref. 71. [g] Ref. 72, NHE = SHE + 6 mV. [h] Ref. 73. [i] Ref. 68.

and, simultaneously, in suppressing the side-reactions of the radical cation.[69]

3. Conclusions

In conclusion, we have studied a water soluble Pt(II)–porphyrin and demonstrated its use as a visible-light driven photosensitizer for water oxidation in a three-component system with four different WOCs and persulfate as a sacrificial electron acceptor in neutral phosphate buffer solution. In some cases, increasing excitation power did not improve the rate of oxygen generation. The overall conversion is probably limited by the rate of the catalytic reaction. The relatively high reduction potentials of the radical cations of Pt(II)–porphyrins allow these chromophores to be used to study a broad range of WOCs with overpotentials $\eta <$ 0.6 V in neutral phosphate buffer solution. More importantly, Pt(II)–TCPP is much more photostable than $Ru(bpy)_3^{2+}$ in phosphate buffer solution during light-driven water oxidation. Whereas these two sensitizers (Pt(II)-TCPP and $Ru(bpy)_3^{2+}$) are both quite photostable in phosphate buffer when excited in the absence of other reagents; the addition of persulfate is very detrimental for $Ru(bpy)_3^{2+}$ (see Fig. S11–S13†). For Pt(II)–TCPP in neutral phosphate buffer solution, the anionic charges of the carboxylate groups have an important stabilizing effect on the π-cation of the oxidized porphyrin.[18,63]

Pt(II)–TCMePP has three times the photon capture ability and 240 mV more oxidizing power than the extensively used $Ru(bpy)_3^{2+}$. Therefore, the Pt(II)–porphyrin is highly suitable as a photoanode for solar water-splitting photoelectrochemical devices. The fabrication of Pt(II)–porphyrin based organic photovoltaic and dye sensitized photoelectrochemical cells is in progress in our laboratory. Moreover, further improvements of the photostability of metal–porphyrin photosensitizers for light-driven water oxidation by rational tuning of the molecular excited state and redox properties are being investigated.

Acknowledgements

This work is part of the research programme of the Foundation for Fundamental Research on Matter (FOM), which is part of the Netherlands Organisation for Scientific Research (NWO). This research is financed in part by the BioSolar Cells open innovation consortium, supported by the Dutch Ministry of Economic Affairs, Agriculture and Innovation and by NWO-Chemical Sciences (CW), VENI grant 700.59.410.

References

1 T. R. Cook, D. K. Dogutan, S. Y. Reece, Y. Surendranath, T. S. Teets and D. G. Nocera, *Chem. Rev.*, 2010, **110**, 6474–6502.
2 N. Armaroli and V. Balzani, *Angew. Chem., Int. Ed.*, 2007, **46**, 52–66.
3 S. Bensaid, G. Centi, E. Garrone, S. Perathoner and G. Saracco, *ChemSusChem*, 2012, **5**, 500–521.
4 D. Gust, T. A. Moore and A. L. Moore, *Acc. Chem. Res.*, 2009, **42**, 1890–1898.
5 M. G. Walter, E. L. Warren, J. R. McKone, S. W. Boettcher, Q. Mi, E. A. Santori and N. S. Lewis, *Chem. Rev.*, 2010, **110**, 6446–6473.
6 B. van den Bosch, H.-C. Chen, J. I. van der Vlugt, A. M. Brouwer and J. N. H. Reek, *ChemSusChem*, 2013, **6**, 790–793.
7 X.-Y. Yang, G. Tian, N. Jiang and B.-L. Su, *Energy Environ. Sci.*, 2012, **5**, 5540–5563.
8 P. D. Tran, L. H. Wong, J. Barber and J. S. C. Loo, *Energy Environ. Sci.*, 2012, **5**, 5902–5918.
9 A. Badura, T. Kothe, W. Schuhmann and M. Rögner, *Energy Environ. Sci.*, 2011, **4**, 3263–3274.
10 G. F. Moore and G. W. Brudvig, *Annu. Rev. Condens. Matter Phys.*, 2011, **2**, 303–327.
11 J. L. Dempsey, B. S. Brunschwig, J. R. Winkler and H. B. Gray, *Acc. Chem. Res.*, 2009, **42**, 1995–2004.
12 L. Duan, L. Tong, Y. Xu and L. Sun, *Energy Environ. Sci.*, 2011, **4**, 3296–3313.
13 D. Shevchenko, M. F. Anderlund, A. Thapper and S. Styring, *Energy Environ. Sci.*, 2011, **4**, 1284–1287.
14 S. Berardi, G. La Ganga, M. Natali, I. Bazzan, F. Puntoriero, A. Sartorel, F. Scandola, S. Campagna and M. Bonchio, *J. Am. Chem. Soc.*, 2012, **134**, 11104–11107.
15 K. Henbest, P. Douglas, M. S. Garley and A. Mills, *J. Photochem. Photobiol., A*, 1994, **80**, 299–305.
16 A. Harriman, G. Porter and P. Walters, *J. Chem. Soc., Faraday Trans. 1*, 1983, 1335–1350.
17 A. Harriman, G. S. Nahor, S. Mosseri and P. Neta, *J. Chem. Soc., Faraday Trans. 1*, 1988, 2821–2829.
18 G. S. Nahor, P. Neta, P. Hambright, A. N. Thompson and A. Harriman, *J. Phys. Chem.*, 1989, **93**, 6181–6187.
19 N. S. McCool, D. M. Robinson, J. E. Sheats and G. C. Dismukes, *J. Am. Chem. Soc.*, 2011, **133**, 11446.
20 L. Duan, Y. Xu, P. Zhang, M. Wang and L. Sun, *Inorg. Chem.*, 2010, **49**, 209–215.
21 C. R. Bock, J. A. Connor, A. R. Gutierrez, T. J. Meyer, D. G. Whitten, B. P. Sullivan and J. K. Nagle, *J. Am. Chem. Soc.*, 1979, **101**, 4815–4824.
22 W. F. Wacholtz, R. A. Auerbach and R. H. Schmehl, *Inorg. Chem.*, 1986, **25**, 227–234.
23 K. Kalyanasundaram, *J. Phys. Chem.*, 1982, **86**, 5163–5169.
24 A. Harriman and M. C. Richoux, *J. Phys. Chem.*, 1983, **87**, 4957–4965.
25 G. S. Nahor, S. Mosseri, P. Neta and A. Harriman, *J. Phys. Chem.*, 1988, **92**, 4499–4504.
26 Y. S. Nam, A. P. Magyar, D. Lee, J.-W. Kim, D. S. Yun, H. Park, T. S. Pollom, D. A. Weitz and A. M. Belcher, *Nat. Nanotechnol.*, 2010, **5**, 340–344.
27 Y. Xu, L. Duan, L. Tong, B. Åkermark and L. Sun, *Chem. Commun.*, 2010, **46**, 6506–6508.
28 G. F. Moore, J. D. Blakemore, R. L. Milot, J. F. Hull, H. Song, L. Cai, C. A. Schmuttenmaer, R. H. Crabtree and G. W. Brudvig, *Energy Environ. Sci.*, 2011, **4**, 2389–2392.
29 Y. Xu, A. Fischer, L. Duan, L. Tong, E. Gabrielsson, B. Åkermark and L. Sun, *Angew. Chem., Int. Ed.*, 2010, **49**, 8934–8937.

30 E. A. Karlsson, B.-L. Lee, T. Åkermark, E. V. Johnston, M. D. Kärkäs, J. Sun, Ö. Hansson, J.-E. Bäckvall and B. Åkermark, *Angew. Chem., Int. Ed.*, 2011, **50**, 11715–11718.
31 C. J. Gagliardi, A. K. Vannucci, J. J. Concepcion, Z. Chen and T. J. Meyer, *Energy Environ. Sci.*, 2012, **5**, 7704–7717.
32 S. Romain, L. Vigara and A. Llobet, *Acc. Chem. Res.*, 2009, **42**, 1944–1953.
33 Y. Surendranath, M. Dinca and D. G. Nocera, *J. Am. Chem. Soc.*, 2009, **131**, 2615–2620.
34 Z. Chen, J. J. Concepcion, X. Hu, W. Yang, P. G. Hoertz and T. J. Meyer, *Proc. Natl. Acad. Sci. U. S. A.*, 2010, **107**, 7225–7229.
35 D. Wang and J. T. Groves, *Proc. Natl. Acad. Sci. U. S. A.*, 2013, **110**, 15579–15584.
36 K. S. Joya, N. K. Subbaiyan, F. D'Souza and H. J. M. de Groot, *Angew. Chem. Int. Ed.*, 2012, **51**, 9601–9605.
37 Z. Chen, J. J. Concepcion and T. J. Meyer, *Dalton Trans.*, 2011, **40**, 3789–3792.
38 B. D. Sherman, S. Pillai, G. Kodis, J. Bergkamp, T. E. Mallouk, D. Gust, T. A. Moore and A. L. Moore, *Can. J. Chem.*, 2011, **89**, 152–157.
39 M. W. Kanan and D. G. Nocera, *Science*, 2008, **321**, 1072–1075.
40 Q. Yin, J. M. Tan, C. Besson, Y. V. Geletii, D. G. Musaev, A. E. Kuznetsov, Z. Luo, K. I. Hardcastle and C. L. Hill, *Science*, 2010, **328**, 342–345.
41 M. Hara, C. C. Waraksa, J. T. Lean, B. A. Lewis and T. E. Mallouk, *J. Phys. Chem. A*, 2000, **104**, 5275–5280.
42 P. K. Ghosh, B. S. Brunschwig, M. Chou, C. Creutz and N. Sutin, *J. Am. Chem. Soc.*, 1984, **106**, 4772–4783.
43 N. Kaveevivitchai, R. Chitta, R. Zong, M. El Ojaimi and R. P. Thummel, *J. Am. Chem. Soc.*, 2012, **134**, 10721–10724.
44 W. J. Youngblood, S.-H. A. Lee, Y. Kobayashi, E. A. Hernandez-Pagan, P. G. Hoertz, T. A. Moore, A. L. Moore, D. Gust and T. E. Mallouk, *J. Am. Chem. Soc.*, 2009, **131**, 926–927.
45 J. R. Swierk and T. E. Mallouk, *Chem. Soc. Rev.*, 2013, **42**, 2357–2387.
46 W. F. Finney, E. Wilson, A. Callender, M. D. Morris and L. W. Beck, *Environ. Sci. Technol.*, 2006, **40**, 2572–2577.
47 P. Chen, O. S. Finikova, Z. Ou, S. A. Vinogradov and K. M. Kadish, *Inorg. Chem.*, 2012, **51**, 6200–6210.
48 D. G. H. Hetterscheid and J. N. H. Reek, *Chem. Commun.*, 2011, **47**, 2712–2714.
49 Y. Zhao, E. A. Hernandez-Pagan, N. M. Vargas-Barbosa, J. L. Dysart and T. E. Mallouk, *J. Phys. Chem. Lett.*, 2011, **2**, 402–406.
50 A. Harriman, I. J. Pickering, J. M. Thomas and P. A. Christensen, *J. Chem. Soc., Faraday Trans. 1*, 1988, 2795–2806.
51 R. P. Briñas, T. Troxler, R. M. Hochstrasser and S. A. Vinogradov, *J. Am. Chem. Soc.*, 2005, **127**, 11851–11862.
52 J. Van Houten and R. J. Watts, *J. Am. Chem. Soc.*, 1975, **98**, 4853–4858.
53 N. D. Schley, J. D. Blakemore, N. K. Subbaiyan, C. D. Incarvito, F. D'Souza, R. H. Crabtree and G. W. Brudvig, *J. Am. Chem. Soc.*, 2011, **133**, 10473–10481.
54 G. La Ganga, F. Puntoriero, S. Campagna, I. Bazzan, S. Berardi, M. Bonchio, A. Sartorel, M. Natali and F. Scandola, *Faraday Discuss.*, 2012, **155**, 177–190.
55 P. G. Hoertz, Y.-I. Kim, W. J. Youngblood and T. E. Mallouk, *J. Phys. Chem. B*, 2007, **111**, 6845–6856.
56 F. Jiao and H. Frei, *Angew. Chem., Int. Ed.*, 2009, **48**, 1841–1844.
57 U. Hintermair, S. M. Hashmi, M. Elimelech and R. H. Crabtree, *J. Am. Chem. Soc.*, 2012, **134**, 9785–9795.
58 D. Hong, J. Jung, J. Park, Y. Yamada, T. Suenobu, Y.-M. Lee, W. Nam and S. Fukuzumi, *Energy Environ. Sci.*, 2012, **5**, 7606–7616.
59 F. A. Frame, T. K. Townsend, R. L. Chamousis, E. M. Sabio, T. Dittrich, N. D. Browning and F. E. Osterloh, *J. Am. Chem. Soc.*, 2011, **133**, 7264–7267.
60 M. Richoux, P. Neta, P. A. Christensen and A. Harriman, *J. Chem. Soc., Faraday Trans. 2*, 1986, 235–249.
61 W. S. Johnson, L. Werthemann, W. R. Bartlett, T. J. Brocksom, T. Li, D. J. Faulkner and M. R. Petersen, *J. Am. Chem. Soc.*, 1970, **92**, 743–745.
62 H. Segawa, R. Azumi and T. Shimidzu, *J. Am. Chem. Soc.*, 1992, **114**, 7564–7565.
63 A. Harriman, P. Neta and M. C. Richoux, *J. Phys. Chem.*, 1986, **90**, 3444–3448.
64 Z. Huang, Z. Luo, Y. V Geletii, J. W. Vickers, Q. Yin, D. Wu, Y. Hou, Y. Ding, J. Song, D. G. Musaev, C. L. Hill and T. Lian, *J. Am. Chem. Soc.*, 2011, **133**, 2068–2071.
65 R. E. Blankenship, D. M. Tiede, J. Barber, G. W. Brudvig, G. Fleming, M. Ghirardi, M. R. Gunner, W. Junge, D. M. Kramer, A. Melis, T. A. Moore, C. C. Moser, D. G. Nocera, A. J. Nozik, D. R. Ort, W. W. Parson, R. C. Prince and R. T. Sayre, *Science*, 2011, **332**, 805–809.
66 J. Barber, *Bioelectrochemistry*, 2002, **55**, 135–138.
67 M. T. Whited, P. I. Djurovich, S. T. Roberts, A. C. Durrell, C. W. Schlenker, S. E. Bradforth and M. E. Thompson, *J. Am. Chem. Soc.*, 2011, **133**, 88–96.
68 Y. Gao, X. Ding, J. Liu, L. Wang, Z. Lu, L. Li and L. Sun, *J. Am. Chem. Soc.*, 2013, **135**, 4219–4222.
69 R. A. Marcus, *Angew. Chem., Int. Ed.*, 1993, **32**, 1111–1121.
70 J. M. Dixon, M. Taniguchi and J. S. Lindsey, *Photochem. Photobiol.*, 2005, **81**, 212–213.
71 M. Kobayashi, S. Ohashi, K. Iwamoto, Y. Shiraiwa, Y. Kato and T. Watanabe, *Biochim. Biophys. Acta*, 2007, **1767**, 596–602.
72 V. V. Pavlishchuk and A. W. Addison, *Inorg. Chim. Acta*, 2000, **298**, 97–102.
73 H. Dau and I. Zaharieva, *Acc. Chem. Res.*, 2009, **42**, 1861–1870.